frontiers in Immunology

ORIGINAL RESEARCH
published: 15 May 2020
doi: 10.3389/fimmu.2020.00654

Immunoglobulin G Subclass-Specific Glycosylation Changes in Primary Epithelial Ovarian Cancer

*Marta Wieczorek[1,2], Elena Ioana Braicu[3], Leticia Oliveira-Ferrer[4], Jahid Sehouli[3] and Véronique Blanchard[1]**

[1] Institute of Laboratory Medicine, Clinical Chemistry and Pathobiochemistry, Charité – Universitätsmedizin Berlin, Corporate Member of Freie Universität Berlin, Humboldt-Universität zu Berlin, and Berlin Institute of Health, Berlin, Germany, [2] Department of Biology, Chemistry and Pharmacy, Freie Universität Berlin, Berlin, Germany, [3] Department of Gynecology, Charité – Universitätsmedizin Berlin, Corporate Member of Freie Universität Berlin, Humboldt-Universität zu Berlin, Berlin Institute of Health, NOGGO Group, Berlin, Germany, [4] Department of Gynecology, University Medical Center Hamburg-Eppendorf, Hamburg, Germany

Epithelial ovarian cancer (EOC) was previously shown to be associated with glycosylation changes of total serum and total IgG proteins. However, as a majority of previous studies analyzed released glycan profiles, still little is known about IgG subclass-specific alterations in ovarian cancer. Hence, in this study, we investigated EOC-related glycosylation changes of the three most abundant IgG subclasses, namely, IgG_1, IgG_2 and IgG_3 isolated from sera of 87 EOC patients and 74 age-matched healthy controls. In order to separate IgG_2 and IgG_3, we performed a two-step affinity purification employing Protein A and Protein G Sepharose. After tryptic digestion, IgG glycopeptides were enriched and measured by MALDI-TOF-MS. Finally, EOC-related glycosylation changes were monitored at the level of total agalactosylation, monogalactosylation, digalactosylation, sialylation, bisection and fucosylation, which were calculated separately for each IgG subclass. Interestingly, aside from an EOC-related increase in agalactosylation/decrease in monogalactosylation and digalactosylation observed in all IgG subclasses, some subclass-specific trends were detected. Glycosylation of IgG_1 was found to be most strongly affected in EOC, as it exhibited the highest number of significant differences between healthy controls and EOC patients. Specifically, IgG_1 was the only subclass that showed a significant decrease in sialylation and a significant increase in fucosylation in EOC patients. Interestingly, IgG_2 and IgG_3 that were often investigated collectively in previous studies, were found to have distinct glycosylation patterns. IgG_3 displayed stronger EOC-related increase in agalactosylation/decrease in digalactosylation and was characterized by notably higher sialylation, which consequently decreased in EOC patients. In conclusion, our study indicates that IgG subclasses exhibit subtly distinct glycosylation patterns of EOC-related alterations and that IgG_1 and IgG_3 agalactosylation show the strongest association with CA125, the routine diagnostic marker. Additionally, our results show that simultaneous analyses of IgG_2 and IgG_3 might lead to wrong conclusions as these two subclasses exhibit noticeably different glycosylation phenotypes.

Keywords: IgG subclasses, N-glycopeptides, glycosylation, ovarian cancer, MALDI-TOF-MS

OPEN ACCESS

Edited by:
Catherine Sautes-Fridman, INSERM U1138 Centre de Recherche des Cordeliers, France

Reviewed by:
David Falck, Leiden University Medical Center, Netherlands
Jean-Luc Teillaud, Institut National de la Santé et de la Recherche Médicale (INSERM), France

***Correspondence:**
Véronique Blanchard
veronique.blanchard@charite.de

Specialty section:
This article was submitted to Cancer Immunity and Immunotherapy, a section of the journal Frontiers in Immunology

Received: *10 October 2019*
Accepted: *23 March 2020*
Published: *15 May 2020*

Citation:
Wieczorek M, Braicu EI, Oliveira-Ferrer L, Sehouli J and Blanchard V (2020) Immunoglobulin G Subclass-Specific Glycosylation Changes in Primary Epithelial Ovarian Cancer. Front. Immunol. 11:654. doi: 10.3389/fimmu.2020.00654

INTRODUCTION

Glycosylation of proteins is one of the most common co-translational and post-translational modifications that consists of the covalent attachment of carbohydrate moieties to polypeptide chains. Apart from increasing protein diversity, glycans are known to play a broad range of roles; that is, they govern the folding of nascent polypeptides in the ER, provide protein physicochemical stability and modify their functions. Moreover, they are involved in various biological processes including cell signaling, extracellular interactions and immune responses (1, 2). Consequently, altered protein glycosylation was shown to be associated with numerous inborn and acquired pathological conditions (3, 4).

Among others, glycosylation changes were reported in ovarian cancer (OC), which remains the most lethal gynecological malignancy in women despite decades of research and better understanding of its etiology (5). Its particularly high mortality results from the lack of early diagnostic markers, which leads to late primary diagnosis and 5-year survival rates as low as 29% in advanced-stage patients (6). In the absence of biomarkers able to reliably detect OC at an early, still asymptomatic stage, altered glycosylation of proteins attracted attention as a potential source of complementary screening markers. Hence, in the last decades, OC-related changes in glycosylation of total serum and of individual proteins were broadly investigated by us (7–9) and by other groups (10–13). Since carcinoma development is accompanied by inflammation, we previously analyzed the N-glycosylation profile of acute-phase proteins isolated from serum samples of epithelial ovarian cancer (EOC) patients (14). Obtained glycosylation profiles revealed not only significant quantitative but also qualitative differences between healthy controls and EOC patients. For instance, triantennary N-glycans containing a (1–6) branch and a Lewis^X epitope or tetraantennary N-glycans containing three Lewis^X epitopes were detected only in EOC patients, which demonstrates their diagnostic potential (14).

In the present study, we aimed at further investigating EOC-related glycosylation changes, turning our focus from liver-originating acute-phase proteins to immunoglobulin G (IgG), secreted by activated plasma B cells. Being present at a concentration of 7–18 mg/ml, IgG represents the most abundant glycoprotein in human serum (15). Each IgG molecule consists of two heavy and two light chains that are covalently linked through disulfide bridges to form a tetrameric Y-shaped structure. Functionally, IgG can be divided into two distinctive parts: fragment antigen binding (Fab), responsible for recognizing and binding to specific antigens, and fragment crystallizable (Fc), which exerts effector functions by interacting with complement, Fc-gamma receptors (FcγRs) and neonatal Fc receptor (FcRn) (16). Within the Fc part, each IgG heavy chain carries a single, highly conserved glycosylation site at asparagine 297 that is typically occupied by biantennary N-glycans of complex type (16, 17). A vast majority of Fc N-glycans is core-fucosylated and bears 0–2 galactose residues. Hence, the three most prominent IgG-Fc glycoforms are G0F (no galactose and one core-fucose), G1F (one galactose and one core-fucose) and G2F (two galactoses and one core-fucose). A small proportion of IgG N-glycans can be further extended by the addition of bisecting *N*-acetylglucosamine (GlcNAc, N) and/or sialic acids (S) (17). Multiple studies showed that IgG-Fc N-glycans are necessary for the maintenance of IgG structural stability, quaternary conformation and induction of its effector functions (18–20).

The presence of aberrantly glycosylated IgG antibodies in the circulation of OC patients was described already in 2001 (21). Later, Saldova et al. (10) defined the nature of these alterations, showing that the serum of OC patients contains a higher fraction of IgG carrying agalactosylated N-glycans and, conversely, lower proportions of those carrying monogalactosylated, digalactosylated and sialylated glycan structures. Their observations, based on the analysis of only three OC serum samples, were further validated in bigger cohort studies by Alley et al. (12) and Qian et al. (13), who not only confirmed that OC was associated with a decreased galactosylation and an increased agalactosylation of IgG but also indicated that observed changes, when combined into a ratio, were superior to routinely used CA125 for discrimination between OC and benign gynecological conditions (13). Based on their results, authors proposed that this ratio could act as an adjunct diagnostic marker, which in combination with CA125 could reduce the number of false-positive outcomes. More recently, Ruhaak et al. examined glycosylation profiles of three major immunoglobulins that are IgG, IgA and IgM, in OC patients, showing that alterations of IgG glycosylation are the most capable of discriminating between OC and healthy individuals (22).

Interestingly, even though human IgG occurs as four subclasses, namely, IgG_1, IgG_2, IgG_3 and IgG_4, a vast majority of the above-mentioned studies monitored glycosylation changes only at the level of total IgG, analyzing enzymatically released IgG N-glycans. Even though Ruhaak et al. (22) performed the analysis at the level of tryptic glycopeptides, their study concentrated on finding the best-performing OC classifier rather than revealing IgG subclass-specific glycosylation alterations. Uncovering subclass-specific IgG glycosylation profiles is, however, important since, despite 90% identity of their amino acid sequences, each subclass is unique and varies with regard to antigen binding, triggering effector functions, half-life and placental transport. Particular attention should be given to IgG_3, because its superior affinity to activating FcγRs (i.e., FcγRI, FcγRIIa, FcγRIIIa, and FcγRIIIb) and complement component 1q (C1q) makes it the most potent pro-inflammatory IgG subclass (23). Despite its unique character, analysis of IgG_3 Fc-glycosylation is rarely performed. This might not only be caused by its lower concentration in blood but also by the fact that tryptic IgG_3 glycopeptide containing asparagine 297 shares the same peptide backbone as IgG_2 or IgG_4, depending on the IgG_3 allotype (24).

Therefore, the aim of our study was to investigate the subclass-specific distribution of IgG glycosylation changes in patients suffering from primary EOC. By performing two-step affinity purification, glycosylation profiles of the three most abundant IgG subclasses, namely, IgG_1, IgG_2 and IgG_3, could be determined individually.

MATERIALS AND METHODS

Sample Collection

Ethical approval was obtained from the Charité Institutional Ethics Committee (EA4/073/06) and from the Ethics Committee of the Medical Association of Hamburg (#OB/V/03). Written informed consent was obtained from all study participants. Eighty-seven primary EOC patients and 74 age- and sex-matched healthy controls were enrolled in this study (**Table 1**). Blood withdrawal was performed using clot activator serum tubes (BD Vacutainer, NJ, USA). At first, blood was allowed to clot for 30 min to 2 h at room temperature and then serum was separated by centrifugation at 1,200 g for 15 min. The obtained serum was aliquoted and stored at −80°C until the time of further analysis.

IgG Purification

IgG was isolated from 5 μl of human serum by sequential two-step affinity purification using immobilized Protein A and immobilized Protein G, as described elsewhere (24), with some modifications. Briefly, 30 μl of Protein A Sepharose CL-4B slurry (GE Healthcare, Eindhoven, The Netherlands) was transferred to a 1.5-ml tube containing 400 μl of phosphate-buffered saline (1 × PBS). After the beads settled, the supernatant was discarded and replaced with 400 μl of 1 × PBS, which was repeated one more time. Following washing, the volume was brought up to 400 μl with 1 × PBS and 5 μl of blood serum were added. The sample mixture was incubated under agitation at 650 rpm for 1 h at room temperature. The entire mixture was applied into a shortened 200-μl filter tip. The flow-through was collected and Protein A Sepharose beads were washed with 5 × 200 μl of 1 × PBS and 3 × 200 μl of Milli-Q water. Captured IgG_1, IgG_2 and IgG_4 were eluted with 3 × 100 μl of 100 mM formic acid (Honeywell Fluka, Steinheim, Germany) and evaporated to dryness in a vacuum centrifuge. Protein A Sepharose beads were regenerated by washing with 2 × 100 μl of 100 mM formic acid, 2 × 200 μl of Milli-Q water and 2 × 200 μl of 1 × PBS. The remaining supernatant was then reapplied on the regenerated Protein A Sepharose column and the flow-through was collected. Protein G Sepharose (30 μl of slurry, GE Healthcare, Eindhoven, The Netherlands) was conditioned as described above for Protein A Sepharose and resuspended in the Protein A flow-through. The following incubation, washing and elution steps were performed the same way as described above for Protein A Sepharose. Collected eluates were dried in vacuum centrifuge and stored at −20°C until further analysis.

TABLE 1 | Demographics of the cohorts used in this study.

	Healthy	EOC
No of patients	74	87
Age (mean ± SD)	59.8 ± 11.2	59.5 ± 10.3
CA125 (mean ± SD)	37.2 ± 106.8	929.4 ± 1,482.0

Age is shown in years and CA125 values are shown as kU/L.

SDS-PAGE and Western Blot

Protein A-bound IgG_1, IgG_2 and IgG_4 fraction as well as Protein G-bound IgG_3 fraction were analyzed by sodium dodecyl sulfate polyacrylamide gel electrophoresis (SDS-PAGE) followed by Coomassie Brilliant Blue staining and western blot analysis using a polyvinylidene fluoride (PVDF) membrane, all using standard techniques. SDS-PAGE was performed using 10% acrylamide gel under reducing conditions. The presence of IgG_3 in Protein A- and Protein G Sepharose-bound fractions was assessed by western blot using recombinant anti-human IgG_3 antibody (1:1,000, Abcam, Cambridge, England).

Tryptic Digestion

Dried IgGs were dissolved in 50 μl of 50 mM ammonium bicarbonate (Merck, Darmstadt, Germany) and shaken for 5 min. Lyophilized sequencing-grade modified trypsin (20-μg vial; Promega, Madison, WI) was dissolved in 100 μl of ice-cold resuspension buffer provided by the manufacturer to obtain a final concentration of 0.2 μg/μl. Five microliters of the solution, corresponding to 1 μg of trypsin, were added to each IgG sample, followed by overnight incubation at 37°C. On the following day, digested IgGs were dried out in a vacuum centrifuge and stored at −20°C until cotton HILIC purification.

Cotton HILIC Purification

IgG glycopeptides were enriched using self-made micro-spin cotton HILIC columns as described elsewhere (25), with minor modifications. Briefly, 10-μl filter tips (Greiner Bio-One, Kremsmünster, Austria) were filled with fibers of cotton wool pads and conditioned by washing with 3 × 50 μl of Milli-Q water and 3 × 50 μl of 80% ACN. Afterward, dried IgG samples were resuspended in 50 μl of 80% ACN and loaded on the self-made microcolumns. They were washed with 3 × 50 μl of 80% ACN containing 0.1% TFA and then with 3 × 50 μl of 80% ACN. The retained IgG glycopeptides were eluted with 6 × 50 μl Milli-Q water, dried out in a vacuum centrifuge and stored at −20°C until MALDI-TOF-MS measurements.

MALDI-TOF-MS Measurements and Data Processing

Dried IgG glycopeptide samples were dissolved in Milli-Q water, and 1 μl was spotted on the stainless-steel MALDI target plate (Bruker Daltonics, Bremen, Germany). Once dried, the sample was overlaid with 1 μl of 2.5 mg/ml 4-chloro-α-cyanocinnamic acid (ClCCA, Sigma-Aldrich, Germany) in 70% ACN and allowed to air-dry at room temperature. All measurements were performed on an Ultraflex III mass spectrometer (Bruker Daltonics, Bremen, Germany) equipped with a Smart Beam laser (laser frequency 100 Hz). Prior to measurement, the mass spectrometer was calibrated with Peptide Calibration Standard II (Bruker Daltonics, Bremen, Germany). Spectra were recorded in reflectron negative ionization mode within the m/z window from 1,000 to 5,000. For each mass spectrum, 5,000 laser shots were accumulated using a partial "random-walk" laser movement mode. Raw mass spectra were exported as ASCII text files, and the subsequent processing that included recalibration,

baseline subtraction and peak extraction was performed with the MassyTools software (26). Recalibration was performed using the list of six IgG_1 glycopeptides (G0F, G1F, G0FN, G2F, G1FN and G2FS1) for mass spectra of Protein A Sepharose-bound IgG or the list of six IgG_3 glycopeptides (G0F, G1F, G0FN, G2F, G1FN and G2FS1) for mass spectra of Protein G Sepharose-bound IgG. The absolute intensities of the detected glycopeptides were normalized to the total area for IgG_1, IgG_2 and IgG_3. Then, by summing up relative intensities of respective glycopeptide structures, six (or five in case of IgG_2) derived glycosylation traits, namely, agalactosylation, monogalactosylation, digalactosylation, sialylation, bisecting GlcNAc and fucosylation, were calculated separately for each IgG subclass, according to the formulas listed below:

Agalactosylation (Agal) = G0F + G0FN + G0 + G0N + mono G0F;
Monogalactosylation (Monogal) = G1F + G1FN + G1FS1 + G1 + G1N + G1S1 + mono G1F;
Digalactosylation (Digal) = G2F + G2FN + G2FS1 + G2 + G2N + G2S1;
Sialylation (Sial) = G1FS1 + G2FS1 + G1S1 + G2S1;
Bisecting GlcNAc (Bisec) = G0FN + G1FN + G2FN + G0N + G1N + G2N;
Fucosylation (Fuc) = G0F + G1F + G2F + G0FN + G1FN + G2FN + G1FS1 + G2FS1 + mono G0F + mono G1F.
Fucosylation of IgG_2 was not evaluated in this study, as most of its afucosylated glycopeptides could not be determined due to the *m/z* overlap with fucosylated glycopeptides of IgG_4. Schematic representation of all detected structures can be found in **Table 2**.

To determine inter-day reproducibility of an applied workflow, the entire analytical procedure, including two-step IgG purification, tryptic digestion, cotton HILIC enrichment, and MALDI-TOF-MS measurement, was repeated using the same serum sample on three consecutive days. Mean, SD and CV values were calculated for six of the most abundant glycopeptide structures of IgG_1, IgG_2 and IgG_3. Results of reproducibility testing are presented in **Supplementary Figure S2**.

Statistical Analysis

Statistical analyses were performed with SPSS version 25.0 (SPSS Inc., Chicago, IL). Means and SD values of IgG_1, IgG_2 and IgG_3 glycosylation traits in healthy controls and EOC patients were calculated and are shown in **Supplementary Table S1** and, in a form of bar graphs, in **Figure 2**. In order to assess associations between IgG glycosylation traits and EOC and to test whether detected EOC-related differences were statistically significant, a regression model was generated for each glycosylation trait. To minimize the effect of age on IgG glycosylation (27, 28), all regression models were corrected by including age as a covariate, which resulted in the following formulas: "glycosylation trait Y $\sim \beta_1$ * patient's status (0 = healthy control, 1 = EOC patient) + β_2 * age + error". Descriptive statistics of all regression models, that is, regression beta coefficients (β), 95% confidence intervals (95% CI) and *p*-values, are listed in **Table 3**. In the following parts of this work, β_1 and p_1 values correspond to EOC-related association, whereas β_2 and p_2 indicate age-related association. After Bonferroni correction for glycosylation traits, *p*-values smaller than or equal to 0.008 (for IgG_1 and IgG_3; 0.05/6 glycosylation traits) and 0.01 (for IgG_2; 0.05/5 glycosylation traits) were considered as statistically significant. Additionally, for each IgG subclass, the relation between agalactosylation and CA125 diagnostic marker (log-transformed values) was assessed by fitting a linear regression model according to the formula "IgG agalactosylation $\sim \beta$ * CA125 + error". Linear graphs with coefficient of determination (R^2), β coefficients and *p*-values are presented in **Figure 3**. For each regression model, the distribution of residuals was inspected and found to be normal.

RESULTS

In the present study, we analyzed the glycosylation profile of the three most abundant IgG subclasses, namely, IgG_1, IgG_2 and IgG_3, in serous EOC patients and age-matched healthy controls by means of MALDI-TOF-MS. Glycosylation analysis was performed at the level of tryptic glycopeptides in order to obtain subclass-specific information. For this purpose, IgG was isolated from serum using two-step affinity purification employing, first, Protein A Sepharose that captures IgG_1, IgG_2 and IgG_4, then Protein G Sepharose in order to bind the IgG_3 contained in the Protein A Sepharose flow-through. Since the amino acid sequence of IgG_2 and IgG_3 glycopeptides are quite often identical (24, 29), the complete depletion of IgG_2 in the first purification step is essential for the subsequent analysis of IgG_3-specific glycosylation. As depicted in **Supplementary Figure S1A**, residual IgG_1, IgG_2 and IgG_4 were removed from the flow-through fraction by its repeated loading on the regenerated Protein A column. The applied procedure allowed the complete binding of IgG_1, IgG_2 and IgG_4, leaving only IgG_3, which is of higher mass, in the flow-through fraction (**Supplementary Figure S1B**). In addition, the contamination of the Protein A Sepharose-bound fraction with the IgG_3 subclass was found to be only minimal and hence negligible as judged by western blot analysis (**Supplementary Figure S1C**).

Captured IgG fractions were digested with trypsin, which generates the following peptide sequences: EEQYNSTYR in IgG_1, EEQFNSTFR in IgG_2/IgG_3 and EEQFNSTYR in IgG_4, where asparagine (N) is occupied by covalently linked N-glycans. Prior to MALDI-TOF-MS measurements, obtained glycopeptides were enriched using self-made cotton HILIC columns (25). Eventually, measurements were performed in negative-ionization mode to enable the simultaneous detection of neutral and underivatized negatively charged (sialylated) IgG glycopeptides. The exemplary MALDI-TOF mass spectra of Protein A- and Protein G-bound fractions are presented in **Figure 1**, whereas all detected structures included in the IgG glycopeptide analysis are listed in **Table 2**. In total, we were able to detect 17 peaks corresponding to IgG_1 glycopeptides, 11 peaks of IgG_2 glycopeptides and 16 peaks of IgG_3 glycopeptides. IgG_4 glycopeptides were not investigated due to very low signals and *m/z* overlap with some afucosylated structures of the more abundant IgG_2 glycopeptides (24). In case

TABLE 2 | Tryptic glycopeptides of human IgG_1, IgG_2 and IgG_3 detected in this study.

Structure composition		*m/z* [M-H]⁻ of detected glycoforms		
		IgG1 (EEQYNSTYR)	IgG2 (EEQFNSTFR)	IgG3 (EEQFNSTFR)
G0F	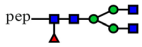	2,632.04	2,600.04	2,600.04
G1F	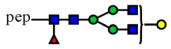	2,794.09	2,762.09	2,762.09
G2F	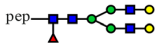	2,956.14	2,924.15	2,924.15
G0FN	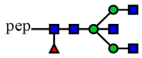	2,835.12	2,803.12	2,803.12
G1FN	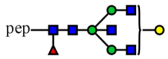	2,997.17	2,965.17	2,965.17
G2FN	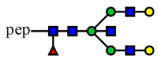	3,159.22	3,127.23	3,127.23
G1FS1		3,085.18	3,053.19	3,053.19
G2FS1		3,247.24	3,215.24	3,215.24
Mono G0F		2,428.96	–	–
Mono G1F	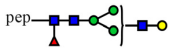	2,591.01	–	–
G0	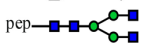	2,485.98	2,453.98	2,453.98
G1	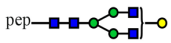	2,648.03	–*	2,616.04
G2	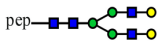	2,810.08	–*	2,778.09
G0N	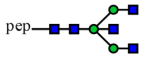	2,689.06	2,657.06	2,657.06
G1N	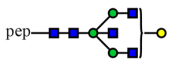	2,851.11	–*	2,819.12
G2N	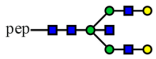	3,013.16	–*	2,981.17
G1S1		–	2,907.13	2,907.13
G2S1	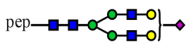	3,101.18	–*	3,069.18

*Schematic representations are given in terms of a pink diamond (sialic acid), yellow circle (galactose), blue square (N-acetylglucosamine), green circle (mannose), red triangle (fucose) and pep (peptide moiety). Structural composition is given in terms of G (galactose), F (fucose), N (bisecting GlcNAc), S (sialic acid), Mono (monoantennary). *Isomeric glycopeptide species of IgG_2 and IgG_4.*

of IgG_1 and IgG_3, glycopeptides carrying both core-fucosylated and afucosylated N-glycans were analyzed. In turn, due to the above-mentioned *m/z* overlap with fucosylated IgG_4 structures (24), a majority of IgG_2 glycopeptides carrying afucosylated N-glycans could not be determined and hence were not taken into account during data analysis. Nevertheless, considering that core-fucosylated structures were shown to constitute on average 97% of all IgG_2 glycoforms (30), exclusion of afucosylated structures has only a minor impact on the entire analysis. Almost all detected glycopeptides carried biantennary complex-type N-glycans bearing zero to two galactoses. Minor amounts of glycopeptides were additionally occupied by bisecting GlcNAc and/or sialic acid.

Since IgG glycosylation is known to vary with age (27, 28), the significance of EOC-related changes was determined with the help of regression models, considering age as a covariate. As visible in **Table 3**, most of the investigated glycosylation traits indeed showed a significant association with age. Consistent with previous studies (31, 32), in all IgG subclasses, agalactosylation was observed to positively correlate with age, whereas monogalactosylation, digalactosylation and sialylation showed a negative correlation, as judged by their respective β coefficient values. Interestingly, glycosylation of IgG_1 was found to be the least affected by age, as only three glycosylation traits (agalactosylation, digalactosylation and sialylation) showed a significant association. On the contrary, in the case of IgG_3, a significant association with age was observed for nearly all glycosylation traits, with fucosylation being the only trait, whose *p*-value (p_2 = 0.009) exceeded the Bonferroni-corrected threshold of α = 0.008 (0.05/6 glycosylation traits), deeming the association insignificant.

IgG_1 Profiling

Among all three subclasses, the glycosylation profile of IgG_1 was found to be the most markedly altered in EOC patients. As visible in **Figure 2** and **Table 3**, IgG_1 exhibited the most pronounced increase in agalactosylation (β_1 = 11.285, p_1 = 1.3E−9) and the most pronounced decrease in monogalactosylation and

TABLE 3 | Associations between IgG glycosylation traits, EOC and age.

Glycosylation trait		IgG1			IgG2			IgG3		
		β	95% CI	*p*	β	95% CI	*p*	β	95% CI	*p*
Agal	(1) EOC	11.285	7.831, 14.738	**1.3E−9**	6.056	2.737, 9.374	**4.2E−4**	9.120	5.242, 12.998	**7.6E−6**
	(2) Age	0.418	0.256, 0.580	**9.9E−7**	0.524	0.369, 0.680	**4.4E−10**	0.609	0.428, 0.789	**5.7E−10**
Monogal	(1) EOC	−5.690	−7.630, −3.750	**3.6E−8**	−3.591	−5.666, −1.516	**8.0E−4**	−3.516	−5.369, −1.663	**2.6E−4**
	(2) Age	−0.118	−0.209, −0.027	0.011	−0.260	−0.357, −0.163	**4.2E−7**	−0.162	−0.249, −0.076	**3.0E−4**
Digal	(1) EOC	−5.596	−7.466, −3.726	**2.0E−8**	−2.465	−3.927, −1.003	**1.1E−3**	−5.604	−8.216, −2.992	**4.0E−5**
	(2) Age	−0.299	−0.387, −0.212	**2.8E−10**	−0.264	−0.333, −0.196	**2.3E−12**	−0.446	−0.568, −0.325	**2.5E−11**
Sial	(1) EOC	−0.576	−0.949, −0.202	**0.003**	−0.052	−0.644, 0.539	0.861	−2.360	−4.229, −0.492	0.014
	(2) Age	−0.039	−0.057, −0.022	**1.9E−5**	−0.072	−0.100, −0.044	**8.3E−7**	−0.275	−0.362, −0.188	**4.6E−9**
Bisec	(1) EOC	−0.852	−2.141, 0.437	0.193	−0.774	−1.764, 0.215	0.124	−0.564	−1.517, 0.388	0.244
	(2) Age	0.052	−0.008, 0.112	0.091	0.038	−0.009, 0.084	0.110	0.084	0.040, 0.128	**2.7E−4**
Fuc	(1) EOC	1.025	0.403, 1.648	**0.001**	–	–	–	0.459	−1.081, 1.998	0.557
	(2) Age	0.005	−0.024, 0.034	0.721	–	–	–	0.096	0.024, 0.168	0.009

For all glycosylation traits, regression beta coefficients (β) are reported together with their 95% confidence interval (95% CI) and respective p-values (p). Bonferroni corrected p-values smaller than or equal to 0.008 (for IgG_1 and IgG_3; 0.05/6 glycosylation traits) and 0.01 (for IgG_2; 0.05/5 glycosylation traits) were considered as statistically significant and are highlighted in bold. Representations of glycosylation traits are given in terms of Agal (agalactosylation), Monogal (monogalactosylation), Digal (digalactosylation), Sial (sialylation), Bisec (bisecting GlcNAc) and Fuc (core-fucosylation).

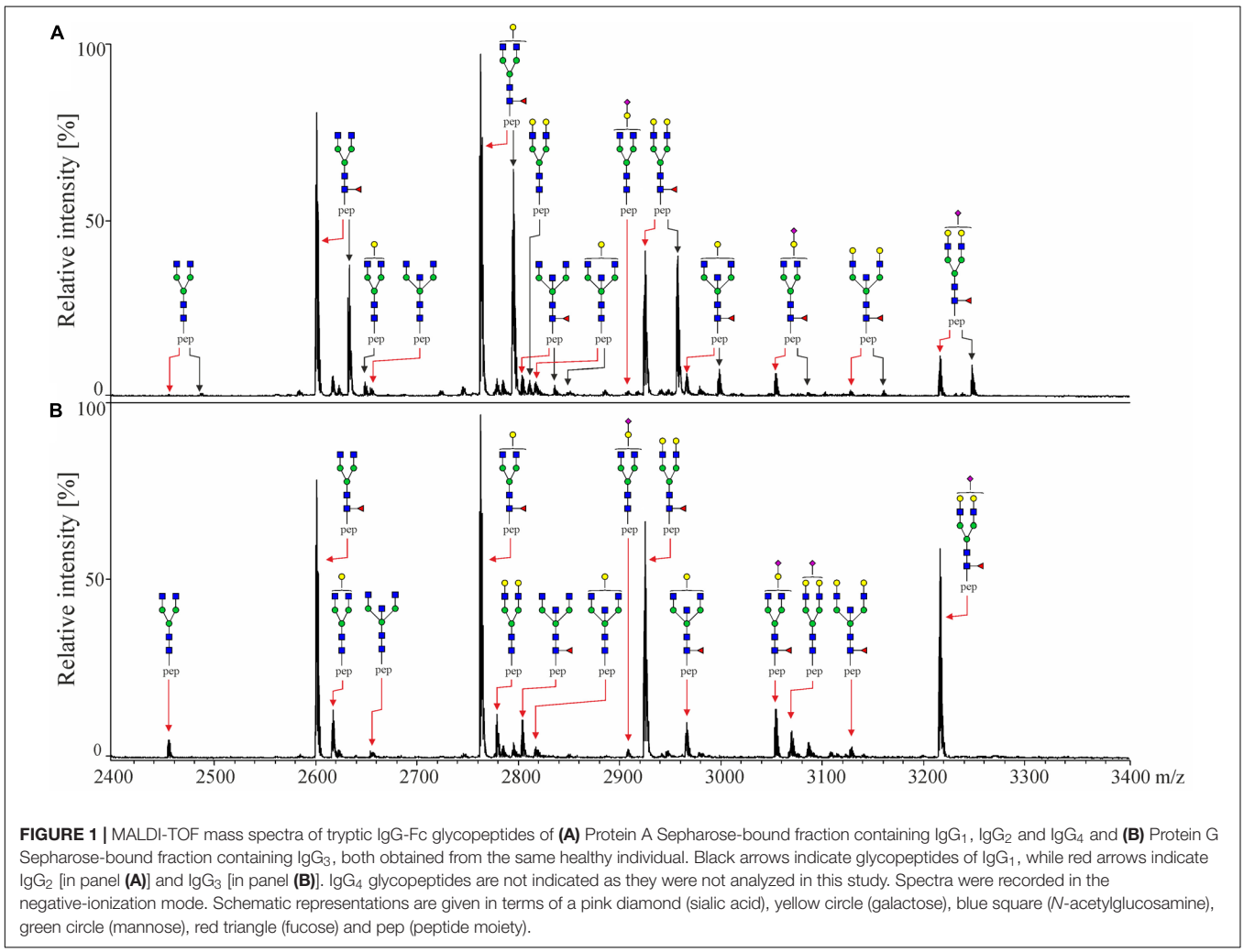

FIGURE 1 | MALDI-TOF mass spectra of tryptic IgG-Fc glycopeptides of **(A)** Protein A Sepharose-bound fraction containing IgG_1, IgG_2 and IgG_4 and **(B)** Protein G Sepharose-bound fraction containing IgG_3, both obtained from the same healthy individual. Black arrows indicate glycopeptides of IgG_1, while red arrows indicate IgG_2 [in panel **(A)**] and IgG_3 [in panel **(B)**]. IgG_4 glycopeptides are not indicated as they were not analyzed in this study. Spectra were recorded in the negative-ionization mode. Schematic representations are given in terms of a pink diamond (sialic acid), yellow circle (galactose), blue square (*N*-acetylglucosamine), green circle (mannose), red triangle (fucose) and pep (peptide moiety).

digalactosylation in EOC patients ($\beta_1 = -5.690$, $p_1 = 3.6E-8$ and $\beta_1 = -5.596$, $p_1 = 2.0E-8$, respectively). Interestingly, even though IgG_1 was found to be characterized by generally low sialylation, it was the only subclass in which sialylation was significantly decreased ($p_1 = 0.003$) in EOC patients. Additionally, IgG_1 was also found to contain the highest proportion of glycopeptides carrying bisecting GlcNAc (**Supplementary Table S1**); however, no significant differences were observed between healthy controls and EOC patients. A vast majority (94–96%) of all detected IgG_1 glycopeptides carried core-fucosylated N-glycans. Remarkably, even though the difference in IgG_1 core-fucosylation between healthy controls and EOC patients was minor (94.5 ± 2.2 in healthy controls versus 95.5 ± 1.8 in EOC patients), the EOC-related increase was found to be statistically significant ($p_1 = 0.001$).

IgG_2 Profiling

EOC-related glycosylation alterations of IgG_2 partially resembled those of IgG_1; however, they were less pronounced (**Figure 2** and **Table 3**). IgG_2 agalactosylation was significantly increased ($\beta_1 = 6.056$, $p_1 = 4.2E-4$), whereas monogalactosylation and digalactosylation were significantly decreased in EOC patients ($\beta_1 = -3.591$, $p_1 = 8.0E-4$ and $\beta_1 = -2.465$, $p_1 = 1.1E-3$, respectively). Interestingly, IgG_2 was found to be characterized by particularly high agalactosylation, which was observed in both investigated groups of individuals. For instance, while in IgG_1 agalactosylation represented 31.6% and 42.7% in healthy controls and EOC patients, respectively, in IgG_2, these were 46.8% and 52.3%, respectively. Hence, on average, IgG_2 agalactosylation was about 12.4% higher in each investigated group. This was further reflected by very low IgG_2 digalactosylation, which constituted only 11.9% in healthy controls and 9.5% in EOC patients (**Supplementary Table S1**). IgG_2 sialylation was slightly higher than in IgG_1; however, no significant differences were detected between healthy controls and EOC patients. Likewise, the abundance of bisecting GlcNAc in IgG_2 was not found to differ between both investigated groups. As mentioned in previous sections, IgG_2 fucosylation was not evaluated in this study due to the *m/z* overlap with fucosylated IgG_4 glycopeptides.

IgG_3 Profiling

Analysis of IgG_3 glycosylation is known to be hindered by its high genetic polymorphism (24, 29). In the Caucasian population, tryptic digestion of IgG_3 usually results in the peptide sequence EEQFNSTFR that is identical to that of IgG_2 (29). However, due to genetic polymorphism, in some individuals, tyrosine replaces phenylalanine at position 296. In this study, 16 samples (i.e., seven healthy controls and nine EOC patients) were excluded from the analysis of the IgG_3 glycosylation due to the presence of different peptide sequences and their resulting glycopeptide moieties, leading to normalization issues. Nonetheless, this did not lead to an age mismatch of investigated groups as the mean age ± SD values remained at 61.6 ± 11.2 years in the healthy group and 59.8 ± 10.3 years in the EOC group, with the difference being statistically insignificant (data not shown). As visible in **Figure 2** and **Table 3**, EOC-related glycosylation changes in IgG_3 resembled those observed in other subclasses; however, they were more pronounced than in IgG_2 and less pronounced than in IgG_1. Agalactosylation of IgG_3 increased in EOC patients ($\beta_1 = 9.120$, $p_1 = 7.6E-6$), whereas monogalactosylation and digalactosylation decreased ($\beta_1 = -3.516$, $p_1 = 2.6E-4$ and $\beta_1 = -5.604$, $p_1 = 4.0E-5$, respectively). Interestingly, IgG_3 was found to be characterized by markedly higher sialylation than in IgG_1 and IgG_2. However, even though its decrease in EOC patients was clearly visible, after Bonferroni correction, the difference between both groups ($p_1 = 0.014$) was deemed statistically insignificant. Both bisecting GlcNAc and fucosylation of IgG_3 showed no significant differences between healthy controls and EOC patients.

Association of IgG Agalactosylation With CA125 Diagnostic Marker

Among all glycosylation traits, IgG agalactosylation displayed the most profound EOC-related alteration. Thus, its association with the most widely used biomarker for OC, namely, CA125, was assessed in the entire cohort using linear regression models. As visible in **Figure 3**, in each IgG subclass, agalactosylation showed a significant positive association with CA125. As judged by R^2 values, β coefficients and *p*-values, the strongest association was observed in IgG_1 ($\beta = 2.793$, $p = 1.7E-8$), whereas the weakest in IgG_2 ($\beta = 1.267$, $p = 0.009$). With an R^2 of 0.074, a β coefficient of 1.856 and a *p*-value of 9.6E−4, IgG_3 displayed a slightly stronger association between its agalactosylation and CA125 than that observed in IgG_2 but weaker than that in IgG_1.

DISCUSSION

In the present study, we investigated the EOC-related glycosylation changes in the three most abundant IgG subclasses, namely, IgG_1, IgG_2 and IgG_3. IgG glycosylation in OC was already examined by several research groups including ours (9, 10, 12, 13, 22), demonstrating quantitative changes in galactosylation/agalactosylation and its utility to improve the detection of OC. Nevertheless, previous studies monitored the glycosylation profile of total IgG at the level of enzymatically released N-glycans. Owing to the fact that about 15–20% of IgG molecules might contain additional N-glycosylation sites within variable domains of Fab fragments, this approach generates information that is neither Fc-/Fab-specific nor subclass-specific. In the present study, analysis of EOC-related changes in IgG glycosylation was performed at the level of tryptic glycopeptides, incorporating an affinity separation of IgG_3 to ensure the subclass specificity of obtained glycosylation profiles and to allow a separate examination of three of the most abundant IgG subclasses.

In accordance with previous OC reports (10, 12, 13, 22), EOC was found to be associated with increased IgG agalactosylation/decreased IgG galactosylation (in this study categorized as monogalactosylation and digalactosylation) in all investigated subclasses. Significantly, these alterations were shown to have relevant biological consequences. Agalactosylated IgG glycoforms are known to act in a pro-inflammatory manner, as they are able to activate the complement system via an

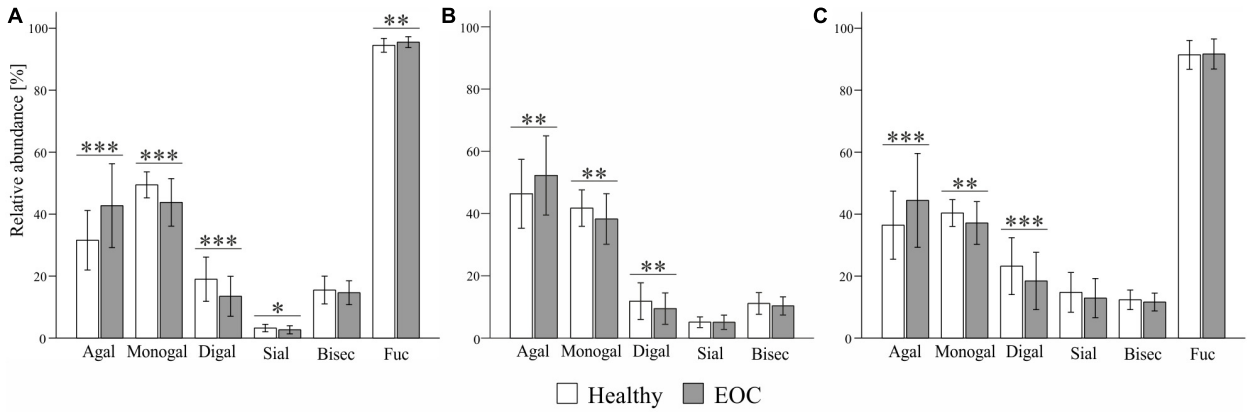

FIGURE 2 | Comparison of **(A)** IgG_1-, **(B)** IgG_2- and **(C)** IgG_3-specific glycosylation profiles between healthy controls and EOC patients. Relative abundance of given glycosylation traits was obtained by summing up relative intensities of the corresponding tryptic glycopeptides detected by MALDI-TOF-MS. Bars represent mean relative abundance and error bars represent standard deviation. *p*-values were obtained from regression analysis, adjusting for age and patients' status (0 = healthy control, 1 = EOC). After Bonferroni correction for glycosylation traits, statistically significant differences are indicated as $^*p \leq 0.008$, $^{**}p \leq 0.001$ and $^{***}p \leq 0.0001$ in case of IgG_1 and IgG_3, and $^*p \leq 0.01$, $^{**}p \leq 0.002$ and $^{***}p \leq 0.0002$ in case of IgG_2.

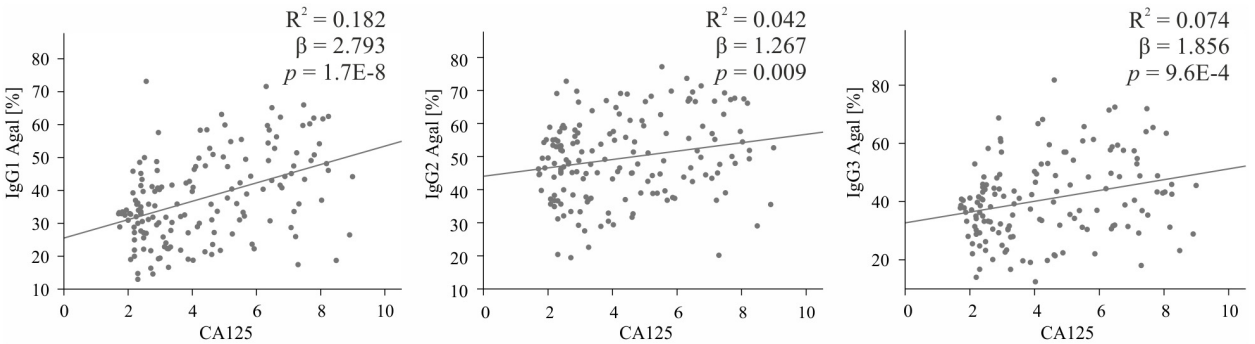

FIGURE 3 | Association between IgG subclass-specific agalactosylation (*Y*-axis) and log (CA125), the routine diagnostic marker (*X*-axis). Descriptive statistics are shown for the total cohort and are given in terms of R^2 (coefficient of determination), β (regression β coefficient) and *p* (*p*-values). IgG_1 is shown on the **left**, IgG_2 in the **middle** and IgG_3 on the **right**.

alternative pathway (33, 34) and the lectin pathway, after binding to mannose-binding lectin (19, 35). Although molecular regulations of the above-described changes are not yet fully understood, in rheumatoid arthritis, a similar trend of reduced IgG galactosylation was shown to result from decreased activity of galactosyltransferase in IgG-producing plasma B cells (36).

Aside from an EOC-related increase in agalactosylation/decrease in galactosylation observed consistently in all investigated IgG subclasses, we detected some distinct subclass-specific trends. Specifically, glycosylation of IgG_1 was found to be the most strongly affected in EOC, and its agalactosylation showed the strongest association with the CA125 diagnostic marker. Our observations are therefore in line with the results of Ruhaak et al. (22), who showed that glycopeptides of this most abundant IgG subclass exhibit the highest diagnostic potential in EOC. Furthermore, our study revealed that IgG_1 undergoes the greatest EOC-related reduction in monogalactosylated and digalactosylated glycopeptides, which might indicate its strongest transformation toward a pro-inflammatory phenotype during EOC development. Interestingly, Saito et al. (37) showed that in gastric cancer patients, a decreased IgG_1 concentration was significantly correlated with a poor prognosis. As the serum concentration of other IgG subclasses showed no relation to patient outcome, authors concluded that IgG_1 must play the most important role in tumor immunity. Remarkably, in our study, IgG_1 was also found to be the only subclass whose fucosylation was significantly increased in EOC patients. Our observations are in agreement with the results of Plomp et al. (30), showing that increased IgG fucosylation is characteristic for individuals with high inflammation, which occurs frequently in OC patients (38). Since IgG core-fucosylation is known to considerably reduce binding to FcγRIIIa and FcγRIIIb receptors, its increase might lead to reduced ADCC activity. As much as this effect may be detrimental to patients, it could be advantageous to cancer by promoting its progression.

Interestingly, the glycosylation profile of IgG_2, marked by particularly low galactosylation, was found to be distinctly

different from that of IgG_1 and IgG_3. This observation implies that a common approach of simultaneous analysis of IgG_2 and IgG_3 might lead to misleading results. IgG_2 was previously reported to exhibit the lowest affinity for FcγRs and the lowest ADCC activity among all IgG subclasses (23, 39). Also, as reported by Plomp et al. (30), IgG_2 glycosylation showed weaker association with markers of inflammation and metabolic health than IgG_1 and IgG_4, indicating its rather limited role in inflammation. Additionally, decreased IgG_2 concentrations were reported in various cancer types, including ovarian, gastric and liver cancer (22, 40, 41), which might indicate that IgG_2 plays a secondary role in cancer development. In line with all those reports, in our study, IgG_2 glycosylation traits showed the weakest association with EOC and the CA125 diagnostic marker.

An essential part of our study was devoted to the investigation of IgG_3-specific glycosylation changes in EOC patients, as to the best of our knowledge, it has not been studied so far. Despite being relatively underrepresented (approximately 5–8% of total IgG), IgG_3 deserves special attention, as in many ways, it is a unique IgG subclass. Its separation can be accomplished due to a particular feature of its amino acid sequence, that is, the presence of arginine instead of histidine at position 435 that prevents its binding to Protein A (42). Moreover, due to its superior affinity toward activating FcγRs and C1q, IgG_3 was shown to be the strongest inducer of Fc-mediated effector functions, including ADCC and CDC (23). Despite its discrete character, glycosylation of IgG_3 is rarely determined individually. Instead, it is investigated in combination with IgG_2, which, as shown in our study, has a markedly different glycosylation profile. Indeed, in terms of glycosylation and EOC-related glycosylation changes, IgG_3 was found to more closely resemble IgG_1 than IgG_2.

Interestingly, even though an observed EOC-related decrease in IgG_3 sialylation was statistically insignificant after multiple testing corrections, we could confirm the overall high IgG_3 sialylation when compared to IgG_1 and IgG_2, already reported in the literature (41, 43). Although the molecular regulation of increased IgG_3 sialylation is not completely understood, it could possibly be related to higher accessibility of IgG_3 Fc-attached N-glycans for sialyltransferases due to structural differences within its Fc-part (42). Additionally, it was proposed that elevated IgG_3 sialylation could result from different processing by B-cell-independent sialidases and sialyltransferases present in serum (43, 44). Having in mind that addition of sialic acid acts as a functional switch turning IgG molecule from pro-inflammatory state to an anti-inflammatory state, in physiological conditions (healthy controls), high IgG_3 sialylation could play a protective role by limiting its excessive inflammatory responses. In turn, a decrease of IgG_3 sialylation in EOC patients might indicate a disease-related transformation toward a pro-inflammatory phenotype, a phenomenon that was observed for other cancer types (40, 45).

IgG glycosylation has already been investigated in various cancer types, often revealing associations with patient survival rate, response to therapy and diagnostic markers. For instance, in gastric cancer patients, a high level of digalactosylated IgG_2 glycoforms was shown to be an indicator of better survival (40), whereas an IgG glycosylation-based model proposed by Qin et al. (46) could accurately predict response to neoadjuvant therapy. In turn, in prostate cancer, the ratio of IgG agalactosylated structures to the sum of monogalactosylated and digalactosylated ones strongly correlated with levels of prostate-specific antigen (PSA), which is the most prevalently used prostate cancer biomarker (47). In our study, IgG agalactosylation showed a strong positive association with CA125, the serum routine biomarker. While comparisons between IgG glycosylation and CA125 have already been reported (13, 22), this is the first study showing associations with CA125 in a subclass-specific manner. Interestingly, as agalactosylation of all subclasses was found to significantly associate with the CA125 marker, the strongest relation was observed for IgG_1 and IgG_3.

In line with previous reports (27, 28, 48), glycosylation profiles of all three IgG subclasses were observed to alter with increasing age. Interestingly, when compared to other subclasses, glycosylation of IgG_1, which displayed the most dramatic EOC-related alterations and the strongest association with CA125, was observed to be the least affected by age. This could indicate that age-related glycosylation changes might diminish differences between older healthy controls and EOC patients, thereby hindering disease discrimination.

In conclusion, by analyzing EOC-related glycosylation changes in the three most abundant IgG subclasses separately, our study broadens the current understanding of molecular backgrounds of EOC pathogenesis. Interestingly, while glycosylation alterations of all IgG subclasses were observed to follow similar patterns, EOC-related changes were most pronounced in IgG_1, which might indicate its particularly important role in OC. As subtle subclass-specific characteristics were also detected, our study highlights the importance of independent analysis of IgG subclasses, particularly in respect to IgG_2 and IgG_3 subclasses.

DATA AVAILABILITY STATEMENT

The datasets generated for this study are available on request to the corresponding author.

ETHICS STATEMENT

The studies involving human participants were reviewed and approved by the Charité – Universitätsmedizin Berlin EA4/073/06 and Medical Association of Hamburg #OB/V/03. The patients/participants provided their written informed consent to participate in this study.

AUTHOR CONTRIBUTIONS

VB, EB, and JS contributed to the conception and the design of the study. EB and LO-F coordinated the collection of samples and the database. MW performed the experiments and data analysis. All authors contributed to the manuscript writing and revision, read and approved the submitted version.

FUNDING

This work was financially supported by the Sonnenfeld Foundation (grant to MW and grant for equipment). The costs of publication of this article were defrayed by Charité – Universitätsmedizin Berlin.

ACKNOWLEDGMENTS

We would like to acknowledge the Sonnenfeld Foundation for financial support, Prof. Rudolf Tauber for fruitful discussions and Dipl.-Math. Anne Pohrt for support in statistical analysis.

SUPPLEMENTARY MATERIAL

The Supplementary Material for this article can be found online at: https://www.frontiersin.org/articles/10.3389/fimmu.2020.00654/full#supplementary-material

FIGURE S1 | (A) Schematic representation of two-step IgG affinity isolation from serum using Protein A and Protein G Sepharose. **(B)** Coomassie stained SDS-PAGE gel presenting Protein A Sepharose-bound fraction containing IgG_1, IgG_2 and IgG_4, and Protein G Sepharose-bound fraction containing IgG_3. The band of IgG_3 heavy chain appears higher in the gel due to its higher molecular mass. **(C)** Western blot analysis of (1) Protein A and (2) Protein G Sepharose-bound fractions using anti-human IgG_3 antibody, showing negligible IgG_3 contamination of Protein A-bound fraction.

FIGURE S2 | Inter-day reproducibility of the IgG subclass-specific glycosylation analysis. The entire analytical procedure including two-step IgG purification, tryptic digestion, cotton-HILIC enrichment and MALDI-TOF-MS measurement were repeated using the same serum sample on three consecutive days. Relative intensities are shown for the six most abundant glycopeptide structures of IgG_1, IgG_2 and IgG_3. Average is shown as mean ± SD. Mean CV of six presented glycopeptides were 1.87 (IgG_1), 2.97 (IgG_2) and 3.11 (IgG_3), indicating good reproducibility of the method.

TABLE S1 | Mean relative intensities and SD values of IgG glycosylation traits in healthy controls and EOC patients. Representations of glycosylation traits are given in terms of Agal (agalactosylation), Monogal (monogalactosylation), Digal (digalactosylation), Sial (sialylation), Bisec (bisecting GlcNAc), Fuc (core-fucosylation).

REFERENCES

1. Rudd PM, Elliott T, Cresswell P, Wilson IA, Dwek RA. Glycosylation and the immune system. *Science*. (2001) 291:2370–6.
2. Varki A. Biological roles of glycans. 2nd ed. In: Lowe JB, Esko JD editors. *Essentials of Glycobiology*. New York, NY: Cold Spring Harbor Laboratory Press. (2009).
3. Pinho SS, Reis CA. Glycosylation in cancer: mechanisms and clinical implications. *Nat Rev Cancer*. (2015) 15:540–55. doi: 10.1038/nrc3982
4. Pascoal C, Francisco R, Ferro T, Dos Reis Ferreira V, Jaeken J, Videira PA. CDG and immune response: from bedside to bench and back. *J Inherit Metab Dis*. (2019) 43:90–124. doi: 10.1002/jimd.12126
5. Siegel RL, Miller KD, Jemal A. Cancer statistics, 2019. *CA Cancer J Clin*. (2019) 69:7–34. doi: 10.3322/caac.21551
6. Mathieu KB, Bedi DG, Thrower SL, Qayyum A, Bast RC Jr. Screening for ovarian cancer: imaging challenges and opportunities for improvement. *Ultrasound Obstet Gynecol*. (2018) 51:293–303. doi: 10.1002/uog.17557
7. Biskup K, Braicu EI, Sehouli J, Fotopoulou C, Tauber R, Berger M, et al. Serum glycome profiling: a biomarker for diagnosis of ovarian cancer. *J Proteome Res*. (2013) 12:4056–63. doi: 10.1021/pr400405x
8. Biskup K, Braicu EI, Sehouli J, Tauber R, Blanchard V. The serum glycome to discriminate between early-stage epithelial ovarian cancer and benign ovarian diseases. *Dis Markers*. (2014) 2014:238197. doi: 10.1155/2014/238197
9. Schwedler C, Kaup M, Petzold D, Hoppe B, Braicu EI, Sehouli J, et al. Sialic acid methylation refines capillary electrophoresis laser-induced fluorescence analyses of immunoglobulin G N-glycans of ovarian cancer patients. *Electrophoresis*. (2014) 35:1025–31.
10. Saldova R, Royle L, Radcliffe CM, Abd Hamid UM, Evans R, Arnold JN, et al. Ovarian cancer is associated with changes in glycosylation in both acute-phase proteins and IgG. *Glycobiology*. (2007) 17:1344–56.
11. Saldova R, Wormald MR, Dwek RA, Rudd PM. Glycosylation changes on serum glycoproteins in ovarian cancer may contribute to disease pathogenesis. *Dis Markers*. (2008) 25:219–32.
12. Alley WR Jr, Vasseur JA, Goetz JA, Svoboda M, Mann BF, Matei DE, et al. N-linked glycan structures and their expressions change in the blood sera of ovarian cancer patients. *J Proteome Res*. (2012) 11:2282–300. doi: 10.1021/pr201070k
13. Qian Y, Wang Y, Zhang X, Zhou L, Zhang Z, Xu J, et al. Quantitative analysis of serum IgG galactosylation assists differential diagnosis of ovarian cancer. *J Proteome Res*. (2013) 12:4046–55. doi: 10.1021/pr4003992
14. Weiz S, Wieczorek M, Schwedler C, Kaup M, Braicu EI, Sehouli J, et al. Acute-phase glycoprotein N-glycome of ovarian cancer patients analyzed by CE-LIF. *Electrophoresis*. (2016) 37:1461–7. doi: 10.1002/elps.201500518
15. Gonzalez-Quintela A, Alende R, Gude F, Campos J, Rey J, Meijide LM, et al. Serum levels of immunoglobulins (IgG, IgA, IgM) in a general adult population and their relationship with alcohol consumption, smoking and common metabolic abnormalities. *Clin Exp Immunol*. (2008) 151:42–50. doi: 10.1111/j.1365-2249.2007.03545.x
16. Schroeder HW Jr., Cavacini L. Structure and function of immunoglobulins. *J Allergy Clin Immunol*. (2010) 125:S41–52. doi: 10.1016/j.jaci.2009.09.046
17. Krapp S, Mimura Y, Jefferis R, Huber R, Sondermann P. Structural analysis of human IgG-Fc glycoforms reveals a correlation between glycosylation and structural integrity. *J Mol Biol*. (2003) 325:979–89.
18. Nezlin R, Ghetie V. Interactions of immunoglobulins outside the antigen-combining site. *Adv Immunol*. (2004) 82:155–215. doi: 10.1016/s0065-2776(04)82004-2
19. Arnold JN, Wormald MR, Sim RB, Rudd PM, Dwek RA. The impact of glycosylation on the biological function and structure of human immunoglobulins. *Annu Rev Immunol*. (2007) 25:21–50. doi: 10.1146/annurev.immunol.25.022106.141702
20. Raju TS. Terminal sugars of Fc glycans influence antibody effector functions of IgGs. *Curr Opin Immunol*. (2008) 20:471–8. doi: 10.1016/j.coi.2008.06.007
21. Gercel-Taylor C, Bazzett LB, Taylor DD. Presence of aberrant tumor-reactive immunoglobulins in the circulation of patients with ovarian cancer. *Gynecol Oncol*. (2001) 81:71–6.
22. Ruhaak LR, Kim K, Stroble C, Taylor SL, Hong Q, Miyamoto S, et al. Protein-specific differential glycosylation of immunoglobulins in serum of ovarian cancer patients. *J Proteome Res*. (2016) 15:1002–10. doi: 10.1021/acs.jproteome.5b01071
23. Vidarsson G, Dekkers G, Rispens T. IgG subclasses and allotypes: from structure to effector functions. *Front Immunol*. (2014) 5:520. doi: 10.3389/fimmu.2014.00520
24. Wuhrer M, Stam JC, van de Geijn FE, Koeleman CA, Verrips CT, Dolhain RJ, et al. Glycosylation profiling of immunoglobulin G (IgG) subclasses from human serum. *Proteomics*. (2007) 7:4070–81.
25. Selman MH, Hemayatkar M, Deelder AM, Wuhrer M. Cotton HILIC SPE microtips for microscale purification and enrichment of glycans and glycopeptides. *Anal Chem*. (2011) 83:2492–9. doi: 10.1021/ac1027116
26. Jansen BC, Reiding KR, Bondt A, Hipgrave Ederveen AL, Palmblad M, Falck D, et al. MassyTools: a high-throughput targeted data processing tool for relative quantitation and quality control developed for glycomic and glycoproteomic MALDI-MS. *J Proteome Res*. (2015) 14:5088–98. doi: 10.1021/acs.jproteome.5b00658
27. Parekh R, Roitt I, Isenberg D, Dwek R, Rademacher T. Age-related galactosylation of the N-linked oligosaccharides of human serum IgG. *J Exp Med*. (1988) 167:1731–6.

28. Krištiæ J, Vuèkoviæ F, Menni C, Klariæ L, Keser T, Beceheli I, et al. Glycans are a novel biomarker of chronological and biological ages. *J Gerontol A Biol Sci Med Sci*. (2014) 69:779–89. doi: 10.1093/gerona/glt190
29. Balbín M, Grubb A, de Lange GG, Grubb R. DNA sequences specific for Caucasian G3m(b) and (g) allotypes: allotyping at the genomic level. *Immunogenetics*. (1994) 39:187–93.
30. Plomp R, Ruhaak LR, Uh HW, Reiding KR, Selman M, Houwing-Duistermaat JJ, et al. Subclass-specific IgG glycosylation is associated with markers of inflammation and metabolic health. *Sci Rep*. (2017) 7:12325. doi: 10.1038/s41598-017-12495-0
31. Chen G, Wang Y, Qin X, Li H, Guo Y, Wang Y, et al. Change in IgG1 Fc N-linked glycosylation in human lung cancer: age- and sex-related diagnostic potential. *Electrophoresis*. (2013) 34:2407–16. doi: 10.1002/elps.201200455
32. de Haan N, Reiding KR, Driessen G, van der Burg M, Wuhrer M. Changes in healthy human IgG Fc-glycosylation after birth and during early childhood. *J Proteome Res*. (2016) 15:1853–61. doi: 10.1021/acs.jproteome.6b00038
33. Banda NK, Wood AK, Takahashi K, Levitt B, Rudd PM, Royle L, et al. Initiation of the alternative pathway of murine complement by immune complexes is dependent on N-glycans in IgG antibodies. *Arthritis Rheum*. (2008) 58:3081–9. doi: 10.1002/art.23865
34. Karsten CM, Pandey MK, Figge J, Kilchenstein R, Taylor PR, Rosas M, et al. Anti-inflammatory activity of IgG1 mediated by Fc galactosylation and association of FcgammaRIIB and dectin-1. *Nat Med*. (2012) 18:1401–6.
35. Malhotra R, Wormald MR, Rudd PM, Fischer PB, Dwek RA, Sim RB. Glycosylation changes of IgG associated with rheumatoid arthritis can activate complement via the mannose-binding protein. *Nat Med*. (1995) 1:237–43.
36. Axford JS, Mackenzie L, Lydyard PM, Hay FC, Isenberg DA, Roitt IM. Reduced B-cell galactosyltransferase activity in rheumatoid arthritis. *Lancet*. (1987) 2:1486–8.
37. Saito H, Miyatani K, Kono Y, Murakami Y, Kuroda H, Matsunaga T, et al. Decreased serum concentration of total IgG is related to tumor progression in gastric cancer patients. *Yonago Acta Med*. (2017) 60:119–25.
38. Macciò A, Lai P, Santona MC, Pagliara L, Melis GB, Mantovani G. High serum levels of soluble IL-2 receptor, cytokines, and C reactive protein correlate with impairment of T cell response in patients with advanced epithelial ovarian cancer. *Gynecol Oncol*. (1998) 69:248–52.
39. Bruhns P, Iannascoli B, England P, Mancardi DA, Fernandez N, Jorieux S, et al. Specificity and affinity of human Fcgamma receptors and their polymorphic variants for human IgG subclasses. *Blood*. (2009) 113:3716–25. doi: 10.1182/blood-2008-09-179754
40. Kodar K, Stadlmann J, Klaamas K, Sergeyev B, Kurtenkov O. Immunoglobulin G Fc N-glycan profiling in patients with gastric cancer by LC-ESI-MS: relation to tumor progression and survival. *Glycoconj J*. (2012) 29:57–66. doi: 10.1007/s10719-011-9364-z
41. Yuan W, Sanda M, Wu J, Koomen J, Goldman R. Quantitative analysis of immunoglobulin subclasses and subclass specific glycosylation by LC-MS-MRM in liver disease. *J Proteomics*. (2015) 116:24–33. doi: 10.1016/j.jprot.2014.12.020
42. Shah IS, Lovell S, Mehzabeen N, Battaile KP, Tolbert TJ. Structural characterization of the Man5 glycoform of human IgG3 Fc. *Mol Immunol*. (2017) 92:28–37. doi: 10.1016/j.molimm.2017.10.001
43. Sonneveld ME, Koeleman CAM, Plomp HR, Wuhrer M, van der Schoot CE, Vidarsson G. Fc-glycosylation in human IgG1 and IgG3 is similar for both total and anti-red-blood cell anti-K antibodies. *Front Immunol*. (2018) 9:129. doi: 10.3389/fimmu.2018.00129
44. Jones MB, Oswald DM, Joshi S, Whiteheart SW, Orlando R, Cobb BA. B-cell-independent sialylation of IgG. *Proc Natl Acad Sci USA*. (2016) 113:7207–12. doi: 10.1073/pnas.1523968113
45. Theodoratou E, Thaçi K, Agakov F, Timofeeva MN, Štambuk J, Puèiæ-Bakoviæ M, et al. Glycosylation of plasma IgG in colorectal cancer prognosis. *Sci Rep*. (2016) 6:28098. doi: 10.1038/srep28098
46. Qin R, Yang Y, Chen H, Qin W, Han J, Gu Y, et al. Prediction of neoadjuvant chemotherapeutic efficacy in patients with locally advanced gastric cancer by serum IgG glycomics profiling. *Clin Proteomics*. (2020) 17:4. doi: 10.1186/s12014-020-9267-8
47. Kanoh Y, Mashiko T, Danbara M, Takayama Y, Ohtani S, Egawa S, et al. Changes in serum IgG oligosaccharide chains with prostate cancer progression. *Anticancer Res*. (2004) 24:3135–9.
48. Chen G, Wang Y, Qiu L, Qin X, Liu H, Wang X, et al. Human IgG Fc-glycosylation profiling reveals associations with age, sex, female sex hormones and thyroid cancer. *J Proteomics*. (2012) 75:2824–34. doi: 10.1016/j.jprot.2012.02.001

Conflict of Interest: The authors declare that the research was conducted in the absence of any commercial or financial relationships that could be construed as a potential conflict of interest.